Second Harmonic Generation in AlGaAs-On-Insulator Waveguides

STUART MAY[1,*], MICHAEL KUES[1], MATTEO CLERICI[1], MARC SOREL[1,*]

[1]*School of Engineering, University of Glasgow, Glasgow, G12 8QQ, Scotland*
**Corresponding authors: stuart.may@glasgow.ac.uk, marc.sorel@glasgow.ac.uk*

Received XX Month XXXX; revised XX Month, XXXX; accepted XX Month XXXX; posted XX Month XXXX (Doc. ID XXXXX); published XX Month XXXX

Second harmonic generation is demonstrated for the first time in AlGaAs-on-insulator waveguides at telecom wavelengths. Using this material platform a maximum internal normalised efficiency of 1202±55%$W^{-1}cm^{-2}$ is achieved for a 100fs pulsed excitation wavelength at 1560nm. This finding is important towards enabling new chip-scale devices for sensing, metrology and quantum optics.

Aluminium Gallium Arsenide (AlGaAs) has long been regarded a very effective material for non-linear optical applications. It has been termed the "silicon of nonlinear optics" [1] thanks to its strong second- and third-order non-linear coefficients. Moreover, its bandgap can be easily increased to values above 1.3 eV by varying the percentage of Aluminium, making AlGaAs transparent to wavelengths down to 0.7μm. This effect allows to mitigate the detrimental impact of two-photon absorption at telecommunication wavelengths, typically hindering the use of silicon-based devices for these applications [2].

AlGaAs waveguides are predominantly grown on their native GaAs substrate to ensure the epitaxial growth of high quality heterosturctures. However, one major drawback of GaAs/AlGaAs waveguides lies in the relatively low modal confinement in the vertical direction, which limits the ease by which phase matching or dispersion engineering can be obtained, often resulting in designs with high propagation losses [3,4]. Recently, the integration of an AlGaAs core on a silica cladding layer, i.e. AlGaAs on Insulator or AlGaAs-OI, has proven to be a very promising approach to expand the capabilities of integrated nonlinear optics in AlGaAs waveguides as it combines the superior non-linear properties of AlGaAs with the strong modal confinement offered by a high index-contrast waveguide [5,6].

AlGaAs boasts one of the highest second-order nonlinear coefficients among the optical materials and is therefore ideally suited for integrated frequency conversion applications such as second harmonic generation (SHG) [7,8]. SHG is essential for the generation of visible and UV light from commonly available laser sources in the near infrared (NIR) [9] and finds numerous applications in areas such as, gas sensing [10], metrology [11], and time-resolved spectroscopy [12]. Moreover, efficient second harmonic generation is of particular importance in the context of energy-time entangled photon pair generation, i.e. when the inverse process of spontaneous parametric down-conversion is driven at the second harmonic wavelength [13] .

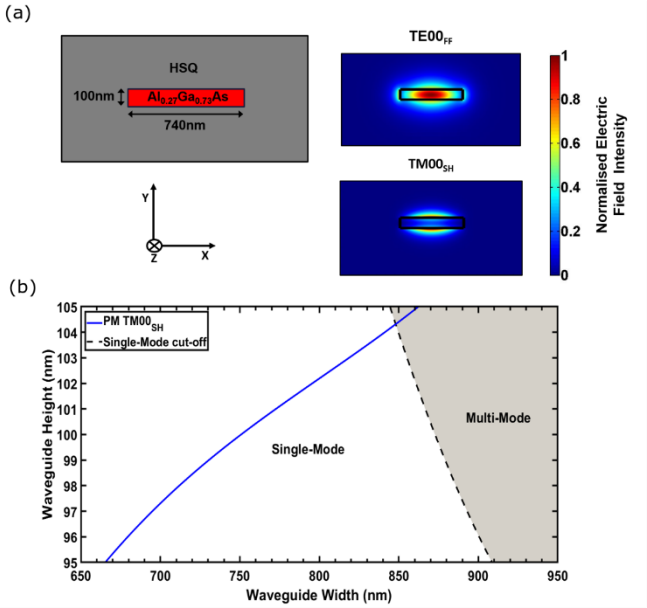

Fig. 1. Phase matching in AlGaAs-OI: (a) Diagram of the waveguide cross-section and the corresponding total electric field intensity of the two modes used for the SHG experiment, where z is the propagation axis into the page (Fundamental Frequency - FF=1560nm, Second Harmonic - SH=780nm) (b) Simulation showing the dimensions of waveguides that provide phase matching (PM) between $TE00_{FF}$ and $TM00_{SH}$ (blue line). The white area of the graph corresponds to the single-mode regime of the waveguide at the FF wavelength, i.e. only $TE00_{FF}$ propagates. The grey area is defined as the multi-mode region of the waveguide, i.e. when higher order modes at the FF wavelength propagate. At the SH frequency the waveguide is multimode for all waveguide dimensions. All simulations were conducted using the Finite Difference Eigenmode Solver (FDE) from Lumerical Inc.

In this letter, we report on the SHG of telecom wavelength laser pulses in an AlGaAs-OI waveguide reaching an internal normalised efficiency of 1202±55%$W^{-1}cm^{-2}$. Since AlGaAs lacks natural birefringence, modal birefringence was employed to guarantee the momentum conservation of participating optical fields, required for efficient frequency conversion.

We designed a waveguide so that it satisfies the phase matching (PM) condition for the generation of the second harmonic: $2\beta_{\mathrm{TE00}}(\omega_{FF}) = \beta_{\mathrm{TM00}}(2\omega_{FF})$, where β is the propagation constant in the waveguide and ω_{FF} is the pump laser's fundamental frequency (FF). Particularly, we considered the PM between the fundamental transverse electric $TE00_{FF}$ mode at the pump wavelength 1560nm, and the fundamental transverse magnetic mode $TM00_{SH}$ at the second harmonic wavelength 780nm. The channel waveguides were comprised of an $Al_{0.27}Ga_{0.73}As$ core, with a Hydrogen silsesquioxane (HSQ, Dow Corning FOX-15) upper and lower cladding, as shown by the waveguide cross-section Fig. 1(a). Upon thermal processing, the HSQ structure becomes a SiO_2-like matrix with a refractive index n~1.39 at 1560nm (verified with ellipsometry), making it ideal for applications at both telecom and visible wavelengths [14,15]. Since a change in the waveguide width and height affect the $TE00_{FF}$ and $TM00_{SH}$ mode dispersion differently, by acting on the two dimensions we found a solution for the phase matching that involves only single mode propagation at 1560nm. To this end a waveguide thickness of 100nm was chosen, and different waveguides with widths ranging from 600 to 900nm were fabricated to guarantee phase matching, as shown in Fig. 1(b).

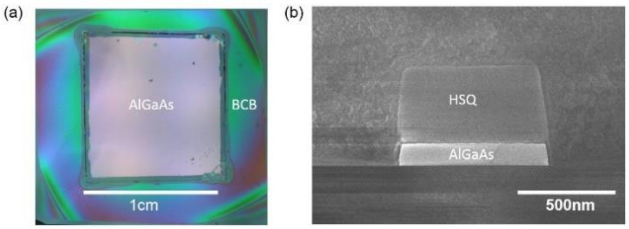

Fig. 2. AlGaAs-OI device images: (a) Optical image of an AlGaAs chip bonded to a Silicon handling sample following substrate and etch stop removal. (b) Scanning Electron Microscope (SEM) image of the cross section of the final AlGaAs-OI waveguide. The average thickness of the waveguide cross-section was measured from the SEM image to be 100.3±1.9nm. The uncertainty in this measurement is predominately dominated by the pixel resolution (1.2nm/pixel), however the standard error in thickness across the width of the waveguide cross-section has also been taken into account.

To fabricate the AlGaAs-OI material platform, HSQ was first spun onto a GaAs-AlGaAs wafer grown via Metal Organic Chemical Vapour Deposition (MOCVD). 3μm of Plasma Enhanced Chemical Vapour Deposition (PECVD) Silica was then deposited on the wafer. These layers act as the Buried oxide (BOX) layer of the final device, thus minimising modal leakage to the Silicon handling substrate. Adhesive sample bonding using Benzocyclobutane (BCB) was subsequently employed to bond the GaAs-AlGaAs with the BOX layer to the Silicon substrate. Pressure was then applied to the samples whilst the BCB was cured at 250°C on a hotplate. Following sample bonding, the GaAs substrate and InGaP etch stops of the GaAs-AlGaAs sample were removed using Citric Acid/Hydrogen peroxide (4:1 volumetric ratio) and HCL acid respectively. This results in the final AlGaAs-OI chip shown in Fig. 2(a). From this platform waveguides were fabricated using Electron Beam lithography to pattern a HSQ hard mask. A $SiCl_4/Ar/N_2$ Inductively Coupled Plasma (ICP) dry etch then transferred this pattern to the AlGaAs before the waveguides were clad in HSQ. A cross section of the final device is shown in Fig. 2(b).

In order to demonstrate and characterize SHG in the AlGaAs-OI waveguides a laser source providing pulses with 100fs duration and repetition rate of 80MHz at a centre wavelength of 1560nm was used. The use of femtosecond pulses for SHG, is of particular importance for the ultrafast optical signal processing [16] , in addition to ultrashort pulse measurement [17] and generation [18,19].

This light was end fire coupled in and out of the AlGaAs-OI waveguides via 40X (NA=0.65) microscope objectives. A combination of low and high pass filters at the output were then used to reject the pump wavelength, before the second harmonic power was measured using a calibrated Silicon biased photodetector. To calculate the average internal power within the waveguide of both the fundamental frequency (FF) and the second harmonic (SH), propagation losses, end facet reflectivity and coupling losses were taken into account. Using the Fabry-Perot loss measurement technique [20], the linear propagation loss at the FF was found to be 14.1±0.3dB/cm. The average coupling loss was ~13.3dB per waveguide facet with reflectivity accounting for approximately 1.4dB of this loss at the FF and 1.6dB at the SH. Taking into consideration these factors, we computed the normalised internal efficiency Γ:

$$\Gamma = \frac{P_{\mathrm{SH}}}{P_{\mathrm{FF}}^2 L^2} \qquad (1)$$

Where P_{SH} and P_{FF} are the average internal power of the fundamental frequency and second harmonic respectively and, L, is the length of the waveguide. Values are commonly quoted in units of $\%W^{-1}cm^{-2}$.

As expected, a clear dependence in the frequency conversion efficiency relative to the waveguide width was observed, demonstrating the effects of phase matching and mismatch, see Fig.3(a). A peak in the normalised internal efficiency was found for waveguide widths from 700 to 780nm. When fabrication tolerances are taken into consideration, this result is in good agreement with the phase matching condition outlined in Fig 1(a), thus confirming phase-matched frequency conversion with AlGaAs-OI for the FF wavelength of 1560nm.

During the final etch stop removal with HCL acid, the average RMS roughness of the waveguide's top surface, i.e. the surface of the AlGaAs layer in Fig.2(a), increased from 0.33nm to 1.10nm (as verified with atomic force microscopy). Since the PM is particularly sensitive to a change in waveguide thickness, see Fig 1(b), this increased surface roughness allows for a wider range of waveguide widths to satisfy the phase matching condition. In turn, this non-uniform thickness along the propagation length of the waveguide resulted in a reduced normalised conversion efficiency.

The high surface roughness was also responsible for a significant increase in propagation losses of frequencies in the SH band because the electric field amplitude of the $TM00_{SH}$ mode is greatest at the top and bottom interface of the waveguide (see Fig 1(a)). Since scattering losses scale with the square of both the modal field at the interface and surface roughness (Payne and Lacey Model, see [21,22]), there is a significant increase in scattering loss

for this mode. Nonlinear losses can be disregarded in this case as applying the scaling laws for multi-photon absorption [23] to measured values, gives a two photon absorption coefficient of $\alpha_{TPA}\approx 0.164 cmGW^{-1}$ [24], and a three photon absorption coefficient of $\alpha_{3PA}\approx 0.055 cm^3GW^{-2}$ [25,26] for $Al_{0.27}Ga_{0.73}As$ at the FF. As a result of these low coefficients, and low intensity of the SH, nonlinear absorption is deemed negligible at both the FF and SH [25]. In sight of this discussion, it was concluded that surface state absorption [27] and scattering were the dominant loss mechanisms for these waveguides, resulting in propagation losses at 780nm comparable to those reported in previous studies on AlGaAs i.e. 200-300dB/cm [28–30]. Since high propagation losses decrease the efficiency of the device, the waveguide length was reduced in order to maximise the output SH power.

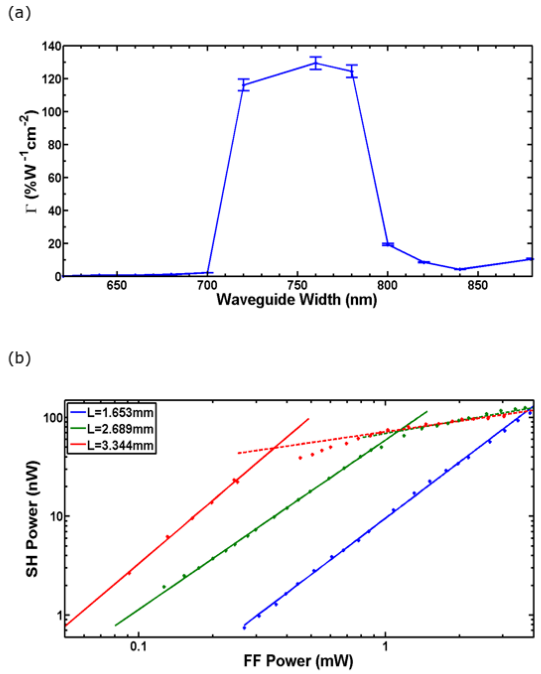

Fig. 3. AlGaAs-OI SHG: (a) Graph showing the phase matching condition for 1.653mm long waveguides of various widths. Average internal FF power=5.1±0.5mW. (b) Logarithmic graph of the average internal FF and SH power of a 700nm wide waveguide of length, L. The gradients of the solid line fits are as follows: 1.89±0.04 (Blue), 1.71±0.02 (Green), 2.13±0.17 (Red). The gradient of the dashed lines are: 0.43±0.07 (Green), 0.36±0.06 (Red).

Another advantage of reducing the waveguide length was the suppression of $\chi^{(3)}$ effects such as self-phase modulation (SPM), which are known to reduce the efficiency of SHG [31]. For low input FF powers, the SH response of the waveguide was found to be quadratic. On a logarithmic scale this gave a gradient of ~2, thus confirming the presence of SHG, see Fig.3(b). As the input power was increased further, third-order effects induced a saturation of the SH power. By reducing the length of the waveguide, the third orders effects, which accumulate along the propagation, were drastically reduced and the threshold for SH saturation increased, as clear from Fig. 3(b). For a waveguide length of 1.653mm, no saturation of the SH was observed up to an average internal FF power of ~3.9mW (peak power ~488W), thus confirming successful repression of $\chi^{(3)}$ effects within the waveguide.

Since $\chi^{(3)}$ nonlinearities cause the phase matching condition for SHG to be intensity dependant, the normalised efficiency will oscillate with both the FF intensity and waveguide length [31]. As a result, the maximum in normalised efficiency was not obtained for the shortest waveguide length but instead for a 2.689mm long waveguide. For a waveguide width of 740nm, a maximum internal normalised efficiency of $1202\pm55\%W^{-1}cm^{-2}$ was measured (see Fig. 4.). As the input power was increased for this waveguide, $\chi^{(3)}$ effects resulted in a decrease in efficiency. Effects such as second harmonic generation cross-phase modulation (SHG-XPM) and Induced phase modulation (IPM), also resulted in clear broadening and modulation of the SH spectra [32,33] –see Fig.5. Since the input pulse spectra spanned from 1485-1620nm, variation in the height of the waveguide also contributed to the broadening of the output SH spectra owing to the phase matching condition being satisfied over a wider range of wavelengths.

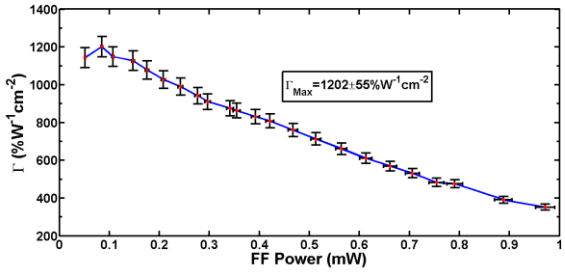

Fig. 4. AlGaAs-OI Normalised Efficiency: Graph of normalised efficiency against average internal FF power of a 740nm wide waveguide (waveguide length= 2.689mm)

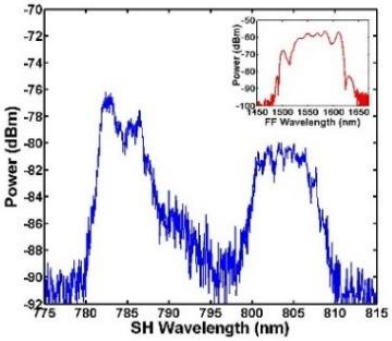

Fig. 5. AlGaAs-OI SH Spectra: Measurement of the output SH spectra of a 740nm wide waveguide (waveguide length= 2.689mm). Average internal FF power=5.6±0.1mW. Red inset shows the input laser pulse spectrum.

The obtained efficiency is comparable to the highest recorded efficiencies for an AlGaAs based material at telecom wavelengths [34], and this result is the first demonstration of SH generation in an AlGaAs-OI chip. Taking into account the group velocity mismatch between the FF and SH mode, and the fact that less than half of the FF spectrum is utilized in the conversion process (Fig.5.), the calculated normalised efficiency is expected to be far greater than

that obtained [35]. The AlGaAs-OI platform also opens up the prospect for further improvement of the SH efficiency through cavity enhancement from a microring resonator [36], making it an ideal platform for SHG.

In conclusion we have demonstrated for the first time the use of AlGaAs-OI for SHG at telecom wavelengths. Using this platform an efficiency of 1202±55%$W^{-1}cm^{-2}$ was obtained. Currently propagation losses are the main limiting factor of this material platform. However, with further optimization of the fabrication process, particularly in obtaining a uniform thickness with low surface roughness [37], or passivation of the top surface, a significant improvement in efficiency can be expected. We speculate that the SH efficiency could be enhanced further, through cavity enhancement from a microring resonator [36] and increase in the temporal and spatial overlap between the FF and SH signals [38,39]. AlGaAs-OI is thus a very promising material platform for wavelength conversion applications such as SH generation and for applications that require both $\chi^{(2)}$ and $\chi^{(3)}$ effects on a single compact integrated chip.

All relevant data present in this publication can be accessed at DOI: https://doi.org/10.5525/gla.researchdata.734

Funding. S.M. and M.S. acknowledge funding from the Engineering and Physical Research Council (EPSRC) (EP/P005624/1) and the Doctoral Training Accounts (DTA). M.K. acknowledges funding from the European Union's Horizon 2020 Research and Innovation programme with the Marie Sklodowska-Curie grant 656607. M.C. acknowledges funding from UKRI (Innovation Fellowship No. EP/S001573/1) and Innovate UK (EP/R043299/1).

Acknowledgment. The authors acknowledge the technical staff at the James Watt Nano-fabrication Centre at Glasgow University.

References

1. G. I. Stegeman, A. Villeneuve, J. Kang, J. S. Aitchison, C. N. Ironside, K. Al-Hemyari, C. C. Yang, C.-H. Lin, H.-H. Lin, G. T. Kennedy, R. S. Grant, and W. Sibbet, J. Nonlinear Opt. Phys. Mater., **3**, 347 (1994).
2. H. K. Tsang, C. S. Wong, T. K. Liang, I. E. Day, S. W. Roberts, A. Harpin, J. Drake, and M. Asghari, Appl. Phys. Lett., **80**, 416 (2002).
3. P. Kultavewuti, V. Pusino, M. Sorel, and J. S. Aitchison, Opt. Lett., **40**, 3029 (2015).
4. N. Morais, I. Roland, M. Ravaro, W. Hease, A.Lemaître, C. Gomez, S. Wabnitz, M. De Rosa, I. Favero, and G. Leo, Opt. Lett., **42**, 4287 (2017).
5. M. Pu, H. Hu, L. Ottaviano, E. Semenova, D. Vukovic, L. Katsuo Oxenløwe, and K. Yvind, Laser Photon. Rev., **12**, 1800111 (2018).
6. H. Hu, F. Da Ros, M. Pu, F. Ye, K. Ingerslev, E. P. da Silva, M. Nooruzzaman, Y. Amma, Y. Sasaki, T. Mizuno, Y. Miyamoto, L.Ottaviano, E. Semenova, P. Guan, D. Zibar, M. Galili, K. Yvind, T. Morioka, and L. Oxenløwe, Nat. Photonics, **12**, 469 (2018).
7. A. Rao and S. Fathpour, Phys. Status Solidi Appl. Mater. Sci., **215**, 1700684 (2018).
8. M. Ohashi, T. Kondo, R. Ito, S. Fukatsu, Y. Shiraki, K. Kumata, and S. S. Kano, J. Appl. Phys., **74**, 596 (1993).
9. E. Garmire, Opt. Express, **21**, 30532 (2013).
10. A. Arie, K. Fradkin-Kashi, and Y. Shreberk, Opt. Lasers Eng., **37**, 159 (2002).
11. T. Udem, R. Holzwarth, and T. W. Hänsch, Nature, **416**, 233 (2002).
12. P. J. Nowakowski, D. A. Woods, C. D. Bain, and J. R. R. Verlet, J. Chem. Phys., **142**, 084201 (2015).
13. L. Caspani, C. Xiong, B. J. Eggleton, D. Bajoni, M. Liscidini, M. Galli, R. Morandotti, and D. J. Moss, Light Sci. Appl., **6**, e17100 (2017).
14. C. W. Holzwarth, T. Barwicz, and H. I. Smith, J. Vac. Sci. Technol. B Microelectron. Nanom. Struct., **25**, 2658 (2007).
15. T. S. Chang, T. C. Chang, P. T. Liu, T. S. Chang, C. H. Tu, and F. S. Yeh, IEEE Electron Device Lett., **27**, 902 (2006).
16. C. Langrock, S. Kumar, J. E. McGeehan, A. E. Willner, and M. M. Fejer, J. Light. Technol., **24**, 2579 (2006).
17. I. Amat-Roldán, I. G. Cormack, P. Loza-Alvarez, E. J. Gualda, and D. Artigas, Opt. Express, **12**, 1169 (2004).
18. E. Sidick, André Knoesen, and A. Dienes, J. Opt. Soc. Am. B, **12**, 1704 (1995).
19. V. Petrov, F. Rotermund, and F. Noack, J. Opt. A Pure Appl. Opt., **3**, R1 (2001).
20. G. Tittelbach, B. Richter, and W. Karthe, Pure Appl. Opt. J. Eur. Opt. Soc. Part A, **2**, 683 (1993).
21. F. P. Payne and J. P. R. Lacey, Opt. Quantum Electron., **26**, 977 (1994).
22. D. Melati, F. Morichetti, and A. Melloni, J. Opt., **16**, 055502 (2014).
23. B. S. Wherrett, J. Opt. Soc. Am. B, **1**, 67 (1984).
24. J. S. Aitchison, D. C. Hutchings, J. U. Kang, G. I. Stegeman, and A. Villeneuve, IEEE J. Quantum Electron., **33**, 341 (1997).
25. J. J. Wathen, P. Apiratikul, C. J. K. Richardson, G. A. Porkolab, G. M. Carter, and T. E. Murphy, Opt. Lett., **39**, 3161 (2014).
26. J. U. Kang, A. Villeneuve, M. Sheik-Bahae, G. I. Stegeman, K. Al-Hemyari, J. S. Aitchison, and C. N. Ironside, Appl. Phys. Lett., **65**, 147 (1994).
27. C. P. Michael, K. Srinivasan, T. J. Johnson, O. Painter, K. H. Lee, K. Hennessy, H. Kim, and E. Hu, Appl. Phys. Lett., **90**, 051108 (2007).
28. L. Scaccabarozzi, M. M. Fejer, Y. Huo, S. Fan, X. Yu, and J. S. Harris, Opt. Lett., **31**, 3626 (2006).
29. D. Duchesne, K. A. Rutkowska, M. Volatier, F. Légaré, S. Delprat, M. Chaker, D. Modotto, A. Locatelli, C. De Angelis, M. Sorel, D. N. Christodoulides, G. Salamo, R. Arès, V. Aimez, and R. Morandotti, Opt. Express, **19**, 12408 (2011).
30. A. Fiore, S. Janz, L. Delobel, P. Van Der Meer, P. Bravetti, V. Berger, E. Rosencher, and J. Nagle, Appl. Phys. Lett., **72**, 2942 (1998).
31. I. A. Begishev, M. Kalashnikov, V. Karpov, P. Nickles, and H. Schönnagel, J. Opt. Soc. Am. B, **21**, 318 (2004).
32. R. R. Alfano, Q. Z. Wang, T. Jimbo, P. P. Ho, R. N. Bhargava, and B. J. Fitzpatrick, Phys. Rev. A, **35**, 459 (1987).
33. P. P. Ho, D. Ji, Q. Z. Wang, and R. R. Alfano, J. Opt. Soc. Am., **7**, 276 (1990).
34. A. S. Helmy, P. Abolghasem, J. Stewart Aitchison, B. J. Bijlani, J. Han, B. M. Holmes, D. C. Hutchings, U. Younis, and S. J. Wagner, Laser Photonics Rev., **5**, 272 (2011).
35. J. B. Han, P. Abolghasem, B. J. Bijlani, A. Arjmand, S. C. Kumar, and A. S. Helmy, J. Opt. Soc. Am. B, **27**, 1291 (2010).
36. Z. Yang, P. Chak, A. D. Bristow, H. M. van Driel, R. Iyer, J. S. Aitchison, A. L. Smirl, and J. E. Sipe, Opt. Lett., **32**, 826 (2007).
37. L. Chang, A. Boes, X. Guo, D. T. Spencer, M. Kennedy, J. D. Peters, N. Volet, J. Chiles, A. Kowligy, N. Nader, D. D. Hickstein, E. J. Stanton, S. A. Diddams, S. B. Papp, and J. E. Bowers, Laser Photonics Rev., **12**, 1800149 (2018).
38. X. Xiao, C. Yang, S. Gao, and H. Miao, IEEE J. Quantum Electron., **41**, 85 (2005).
39. H. Ishikawa and T. Kondo, Appl. Phys. Express, **2**, 0422021 (2009).

Full References

1. G. I. Stegeman, A. Villeneuve, J. Kang, J. S. Aitchison, C. N. Ironside, K. Al-Hemyari, C. C. Yang, C.-H. Lin, H.-H. Lin, G. T. Kennedy, R. S. Grant, and W. Sibbet, "AlGaAs Below Half Bandgap: The Silicon of Nonlinear Optical Materials," J. Nonlinear Opt. Phys. Mater., **3**, 347 (1994).
2. H. K. Tsang, C. S. Wong, T. K. Liang, I. E. Day, S. W. Roberts, A. Harpin, J. Drake, and M. Asghari, "Optical dispersion, two-photon absorption and self-phase modulation in silicon waveguides at 1.5μm wavelength," Appl. Phys. Lett., **80**, 416 (2002).
3. P. Kultavewuti, V. Pusino, M. Sorel, and J. S. Aitchison, "Low-power continuous-wave four-wave mixing wavelength conversion in AlGaAs-nanowaveguide microresonators," Opt. Lett., **40**, 3029 (2015).
4. N. Morais, I. Roland, M. Ravaro, W. Hease, A.Lemaître, C. Gomez, S. Wabnitz, M. De Rosa, I. Favero, and G. Leo, "Directionally induced quasi-phase matching in homogeneous AlGaAs waveguides," Opt. Lett., **42**, 4287 (2017).
5. M. Pu, H. Hu, L. Ottaviano, E. Semenova, D. Vukovic, L. Katsuo Oxenløwe, and K. Yvind, "Ultra-efficient and broadband nonlinear AlGaAs-on-insulator chip for low-power optical signal processing," Laser Photon. Rev., **12**, 1800111 (2018).
6. H. Hu, F. Da Ros, M. Pu, F. Ye, K. Ingerslev, E. P. da Silva, M. Nooruzzaman, Y. Amma, Y. Sasaki, T. Mizuno, Y. Miyamoto, L.Ottaviano, E. Semenova, P. Guan, D. Zibar, M. Galili, K. Yvind, T. Morioka, and L. Oxenløwe, "Single-Source Chip-based Frequency Comb Enabling Extreme Parallel Data Transmission," Nat. Photonics, **12**, 469 (2018).
7. A. Rao and S. Fathpour, "Second-Harmonic Generation in Integrated Photonics on Silicon," Phys. Status Solidi Appl. Mater. Sci., **215**, 1700684 (2018).
8. M. Ohashi, T. Kondo, R. Ito, S. Fukatsu, Y. Shiraki, K. Kumata, and S. S. Kano, "Determination of quadratic nonlinear optical coefficient of AlxGa1-xAs system by the method of reflected second harmonics," J. Appl. Phys., **74**, 596 (1993).
9. E. Garmire, "Nonlinear optics in daily life," Opt. Express, **21**, 30532 (2013).
10. A. Arie, K. Fradkin-Kashi, and Y. Shreberk, "Frequency conversion in novel materials and its application to high resolution gas sensing," Opt. Lasers Eng., **37**, 159 (2002).
11. T. Udem, R. Holzwarth, and T. W. Hänsch, "Optical frequency metrology.," Nature, **416**, 233 (2002).
12. P. J. Nowakowski, D. A. Woods, C. D. Bain, and J. R. R. Verlet, "Time-resolved phase-sensitive second harmonic generation spectroscopy," J. Chem. Phys., **142**, 084201 (2015).
13. L. Caspani, C. Xiong, B. J. Eggleton, D. Bajoni, M. Liscidini, M. Galli, R. Morandotti, and D. J. Moss, "Integrated sources of photon quantum states based on nonlinear optics," Light Sci. Appl., **6**, e17100 (2017).
14. C. W. Holzwarth, T. Barwicz, and H. I. Smith, "Optimization of hydrogen silsesquioxane for photonic applications," J. Vac. Sci. Technol. B Microelectron. Nanom. Struct., **25**, 2658 (2007).
15. T. S. Chang, T. C. Chang, P. T. Liu, T. S. Chang, C. H. Tu, and F. S. Yeh, "Improvement of hydrogenated amorphous-silicon TFT performances with low-κ siloxane-based hydrogen silsesquioxane (HSQ) passivation layer," IEEE Electron Device Lett., **27**, 902 (2006).
16. C. Langrock, S. Kumar, J. E. McGeehan, A. E. Willner, and M. M. Fejer, "All-Optical Signal Processing Using $\chi(2)$ Nonlinearities in Guided-Wave Devices," J. Light. Technol., **24**, 2579 (2006).
17. I. Amat-Roldán, I. G. Cormack, P. Loza-Alvarez, E. J. Gualda, and D. Artigas, "Ultrashort pulse characterisation with SHG collinear-FROG," Opt. Express, **12**, 1169 (2004).
18. E. Sidick, André Knoesen, and A. Dienes, "Ultrashort-pulse second-harmonic generation. I. Transform-limited fundamental pulses," J. Opt. Soc. Am. B, **12**, 1704 (1995).
19. V. Petrov, F. Rotermund, and F. Noack, "Generation of high-power femtosecond light pulses at 1 kHz in the mid-infrared spectral range between 3 and 12 μm by second-order nonlinear processes in optical crystals," J. Opt. A Pure Appl. Opt., **3**, R1 (2001).
20. G. Tittelbach, B. Richter, and W. Karthe, "Comparison of three transmission methods for integrated optical waveguide propagation loss measurement," Pure Appl. Opt. J. Eur. Opt. Soc. Part A, **2**, 683 (1993).
21. F. P. Payne and J. P. R. Lacey, "A theoretical analysis of scattering loss from planar optical waveguides," Opt. Quantum Electron., **26**, 977 (1994).
22. D. Melati, F. Morichetti, and A. Melloni, "A unified approach for radiative losses and backscattering in optical waveguides," J. Opt., **16**, 055502 (2014).
23. B. S. Wherrett, "Scaling rules for multiphoton interband absorption in semiconductors," J. Opt. Soc. Am. B, **1**, 67 (1984).
24. J. S. Aitchison, D. C. Hutchings, J. U. Kang, G. I. Stegeman, and A. Villeneuve, "The nonlinear optical properties of AlGaAs at the half band gap," IEEE J. Quantum Electron., **33**, 341 (1997).
25. J. J. Wathen, P. Apiratikul, C. J. K. Richardson, G. A. Porkolab, G. M. Carter, and T. E. Murphy, "Efficient continuous-wave four-wave mixing in bandgap-engineered AlGaAs waveguides," Opt. Lett., **39**, 3161 (2014).
26. J. U. Kang, A. Villeneuve, M. Sheik-Bahae, G. I. Stegeman, K. Al-Hemyari, J. S. Aitchison, and C. N. Ironside, "Limitation due to threephoton absorption on the useful spectral range for nonlinear optics in AlGaAs below half band gap," Appl. Phys. Lett., **65**, 147 (1994).
27. C. P. Michael, K. Srinivasan, T. J. Johnson, O. Painter, K. H. Lee, K. Hennessy, H. Kim, and E. Hu, "Wavelength- and material-dependent absorption in GaAs and AlGaAs microcavities," Appl. Phys. Lett., **90**, 051108 (2007).
28. L. Scaccabarozzi, M. M. Fejer, Y. Huo, S. Fan, X. Yu, and J. S. Harris, "Enhanced second-harmonic generation in AlGaAs/AlxOy tightly confining waveguides and resonant cavities," Opt. Lett., **31**, 3626 (2006).
29. D. Duchesne, K. A. Rutkowska, M. Volatier, F. Légaré, S. Delprat, M. Chaker, D. Modotto, A. Locatelli, C. De Angelis, M. Sorel, D. N. Christodoulides, G. Salamo, R. Arès, V. Aimez, and R. Morandotti, "Second harmonic generation in AlGaAs photonic wires using low power continuous wave light," Opt. Express, **19**, 12408 (2011).
30. A. Fiore, S. Janz, L. Delobel, P. Van Der Meer, P. Bravetti, V. Berger, E. Rosencher, and J. Nagle, "Second-harmonic generation at λ=1.6 μm in AlGaAs/Al2O3waveguides using birefringence phase matching," Appl. Phys. Lett., **72**, 2942 (1998).
31. I. A. Begishev, M. Kalashnikov, V. Karpov, P. Nickles, and H. Schönnagel, "Limitation of second-harmonic generation of femtosecond Ti:sapphire laser pulses," J. Opt. Soc. Am. B, **21**, 318 (2004).
32. R. R. Alfano, Q. Z. Wang, T. Jimbo, P. P. Ho, R. N. Bhargava, and B. J. Fitzpatrick, "Induced spectral broadening about a second harmonic generated by an intense primary ultrashort laser pulse in ZnSe crystals," Phys. Rev. A, **35**, 459 (1987).
33. P. P. Ho, D. Ji, Q. Z. Wang, and R. R. Alfano, "Second-Harmonic Generation of Ultrashort Laser Pulses in Nonlinear-Optical Media," J. Opt. Soc. Am., **7**, 276 (1990).
34. A. S. Helmy, P. Abolghasem, J. Stewart Aitchison, B. J. Bijlani, J. Han, B. M. Holmes, D. C. Hutchings, U. Younis, and S. J. Wagner, "Recent advances in phase matching of second-order nonlinearities in monolithic semiconductor waveguides," Laser Photonics Rev., **5**, 272 (2011).
35. J. B. Han, P. Abolghasem, B. J. Bijlani, A. Arjmand, S. C. Kumar, and A. S. Helmy, "Femtosecond second-harmonic generation in AlGaAs Bragg reflection waveguides : theory and experiment," J. Opt. Soc. Am. B, **27**, 1291 (2010).
36. Z. Yang, P. Chak, A. D. Bristow, H. M. van Driel, R. Iyer, J. S. Aitchison, A. L. Smirl, and J. E. Sipe, "Enhanced second-harmonic generation in AlGaAs microring resonators," Opt. Lett., **32**, 826 (2007).
37. L. Chang, A. Boes, X. Guo, D. T. Spencer, M. Kennedy, J. D. Peters, N. Volet, J. Chiles, A. Kowligy, N. Nader, D. D. Hickstein, E. J. Stanton, S. A. Diddams, S. B. Papp, and J. E. Bowers,

"Heterogeneously integrated GaAs waveguides on insulator for efficient frequency conversion," Laser Photonics Rev., **12**, 1800149 (2018).
38. X. Xiao, C. Yang, S. Gao, and H. Miao, "Analysis of Ultrashort-Pulse Second-Harmonic Generation in Both Phase- and Group-Velocity- Matched Structures," IEEE J. Quantum Electron., **41**, 85 (2005).
39. H. Ishikawa and T. Kondo, "Birefringent phase matching in thin rectangular high-index-contrast waveguides," Appl. Phys. Express, **2**, 0422021 (2009).